NATURE OF HARD X-RAY SOURCE FROM OPTICAL IDENTIFICATION OF THE ASCA LARGE SKY SURVEY

Masayuki Akiyama
SUBARU Telescope NAOJ, 650 North A'ohoku Place, Hilo, 96720, HI, U.S.A
/ Department of Astronomy, Kyoto University

Kouji Ohta
Department of Astronomy, Kyoto University

Toru Yamada
Astronomical Institute, Tohoku University

Yoshihiro Ueda and Tadayuki Takahashi
ISAS

Masaaki Sakano and Takeshi Tsuru
Department of Physics, Kyoto University

Ingo Lehmann and Günther Hasinger
Astrophysikalisches Institut Potsdam

ABSTRACT

We present results of optical identification of the ASCA Large Sky Survey. X-ray sources which have hard X-ray spectra were identified with type-2 AGN at redshifts smaller than 0.5. It is supported that the absorbed X-ray spectrum of type-2 AGN makes the Cosmic X-ray Background harder in the hard X-ray band than type-1 AGN, which is main contributer in the soft X-ray band. Absence of type-2 AGN at redshift larger than 1 in the identified sample, which contrasts to the existence of 6 broad-line QSOs, suggests a deficiency of so-called "type-2 QSO" at high redshift.

1. Introduction

In order to understand the origin of the Cosmic X-ray Background (CXB), especially to reveal the nature of the hard X-ray sources, which are required to account for the spectrum of the CXB, we are making a wide area X-ray source survey using the ASCA satellite in the 0.7–10 keV band (the ASCA Large Sky Survey hereafter LSS, Ueda et al. 1998a, Ueda et al. 1998b, Ueda et al. 1998c). It covered 7 square degree of the sky near the north galactic pole down to the X-ray flux of 10^{-13} erg/sec/cm^2 in the 2–10 keV band. We have detected 44 sources in the 2–10 keV band above 3.5σ by the GIS and SIS and resolved 23% of the CXB. Significant fraction of detected

X-ray sources had a hard photon index (smaller than 1.0) and the averaged X-ray spectrum of the sources have a photon index of 1.49±0.10 in the 2–10 keV band (Ueda et al. 1998a); closer to that of the CXB ($\Gamma \sim$1.4: e.g., Gendreau et al. 1995) than that of type-1 AGNs ($\Gamma \sim$1.7: e.g., Turner and Pounds 1989), which are the main contributer to the CXB in the 0.5–2 keV ROSAT band (e.g., Schmidt et al. 1998). A good candidate for these hard sources is a type-2 AGN (e.g., Comastri et al. 1995). In this presentation, we summarize the results of optical identification of the LSS. Throughout this paper, we used H_0=50km/sec/Mpc and q_0=0.5.

2. Optical Follow-up Observation of the LSS and reliability of the identification

We have made observations for optical identification of 34 X-ray sources detected above 3.5σ with the SIS in the 2–7 keV band. We selected candidates of optical counterparts using CCD images taken with the KISO Schmidt telescope and the APM catalog (McMahon et al. 1992). For some sources, deep images were obtained with the University of Hawaii 88″ telescope. An error radius of an ASCA source is estimated to be 0.6–0.8 arcmin (Ueda et al. 1998c) and there are some optical objects within each error circle. We have selected targets for spectroscopy using various catalogs and optical color and magnitude as shown below.

1. ROSAT data : We made ROSAT HRI observations of the selected areas (2 fields of HRI). Almost all LSS sources in the field were detected by the HRI and their optical counterparts were pinpointed. ROSAT PSPC source catalog (Voges et al. 1998) was also used for other sources.

2. VLA FIRST catalog (White et al. 1997) : About half (13/34) of the sample were detected in the FIRST survey and optical counterpart was pinpointed thanks to the good positional accuracy of the FIRST catalog. The high fraction of radio-detected source is due to nice match between the limit ($\sim$ 1mJy) of VLA FIRST 1.4 GHz survey and that of the LSS; ratio of the flux limits is comparable to the radio to X-ray flux ratio of *radio-quiet* type-1 AGN (e.g., Elvis et al. 1994). It is worth noting that radio emission is transparent against obscuring material, thus obscured AGNs are unbiasly detected in the radio wavelength as well as hard X-ray. Chance coincidence of a radio source which is not an X-ray counterpart is expected to be 0.5 for the whole sample and is negligible.

3. Optical magnitude, color and galaxy excess : As a type-1 AGN candidate, we selected optical objects using optical magnitude and color (Akiyama et al. 1998a). X-ray sources associated with an excess of galaxies in the optical image were identified with clusters of galaxies.

Most sources have at least one object which meets one of the above criteria. We have made spectroscopic observations for these objects with the highest priority.

Spectroscopic observations were made at the UH 88″ telescope at Mauna Kea. The X-ray sources were identified with 19 type-1 AGNs, 3 type-1.5 AGNs which show a broad Hα but no

broad Hβ line, 6 type-2 AGNs which show AGN-like line ratios and no broad line, 2 clusters of galaxies (not spectroscopically confirmed yet), and one galactic star. 3 sources are still unidentified.

We have checked the reliability of our identification by estimating chance contaminations. Considering number counts of type-1 AGN (Hartwick and Schade 1990), the expected number of chance contaminations of type-1 AGN brighter than B=21.0 with redshift smaller than 3 within 34 error circles is 0.29 and negligible. For type-2 AGNs, 4/6 of them are pinpointed by FIRST radio survey and chance contamination is very small for the sample as mentioned above. One of the remaining type-2 AGNs is pointed out by ROSAT PSPC. Therefore our identifications are reliable.

3. Nature of the Hard Sources

The distribution of the observed photon index as a function of redshift is shown in figure 1. All X-ray sources which have photon index smaller than 1 are identified with type-2 AGNs at redshifts smaller than 0.5. For example, the hardest source was identified with a type-2 Seyfert at z=0.072 (Akiyama et al. 1998b). A dashed line in figure 1 shows an expected change of *apparent* photon index (0.7–10 keV) for a type-1 Seyfert with redshift. Because of the reflection component, observed photon index of a type-1 Seyfert in the 0.7–10 keV band is expected to be getting harder to z$\sim$2. The photon index distribution of the type-1 AGN sample is consistent with this decreasing trend. It should be noted that at larger redshift the apparent photon index turns to larger and will not be as hard as the CXB.

We have derived column densities of absorbing matter at the object's redshift assuming an intrinsic photon index of 1.7 (figure 1 right). The type-2 AGNs which have hard X-ray spectra are fitted with column density of 10^{22} $\sim$$10^{23}$ /cm^2. The upper boundary of the distribution of the column density ($N_H \sim 10^{22.5}$ /cm^2) is consistent with an estimated limit on the column density in the LSS sample (see figure 2). Three high-redshift type-1 AGNs are fitted with large column densities. This can be explained by the effect of the reflection component as shown above.

These results support an idea that the absorbed X-ray spectra of type-2 AGNs make the CXB harder than type-1 AGN (Comastri et al. 1995). However there is no hard X-ray source which identified with object at high redshift. This seems to be inconsistent with the CXB model which assume that the type-1 to type-2 AGN ratio does not change with redshift and luminosity. In the next section we examine the redshift and luminosity distribution of the identified AGNs.

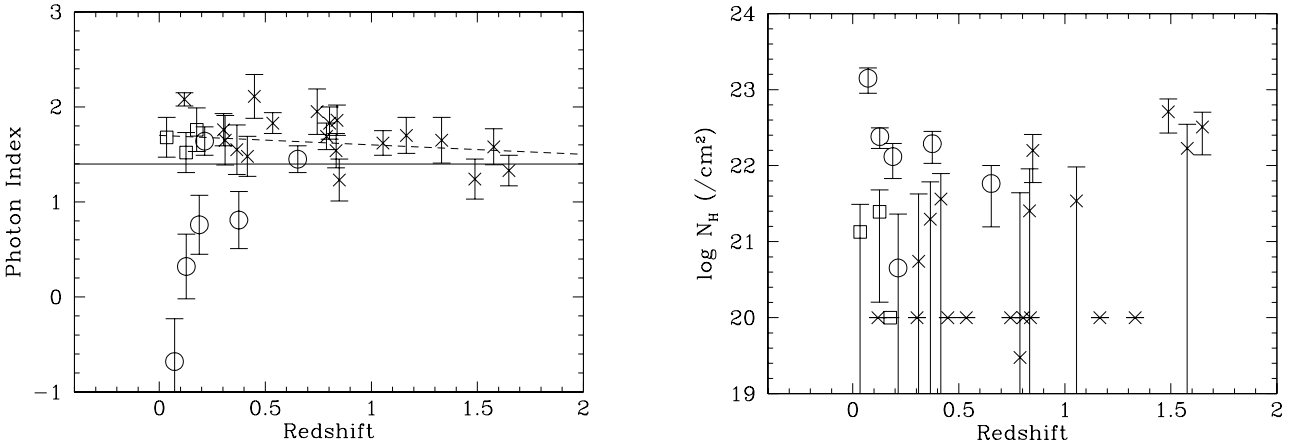

Fig. 1.— Left: Photon index versus redshift of the identified AGNs. Cross, rectangle, and circle represent type-1 AGN, type-1.5 AGN, and type-2 AGN, respectively. Horizontal solid line is the photon index of the CXB. Expected change of apparent photon index (0.7–10 keV) for a type-1 Seyfert with redshift is shown as a dashed line. It is derived by using the average X-ray spectrum of nearby type-1 Seyferts (Gondek et al. 1995). Right: Column density versus redshift. Marks are the same as in the left panel. Fitting is made by assuming an intrinsic photon index of 1.7 and an intrinsic absorption at the object redshift. X-ray sources which have photon index larger than 1.7 is plotted at column density of $10^{20}/\mathrm{cm}^2$. Photon index and column density are determined in the 0.7–10 keV band.

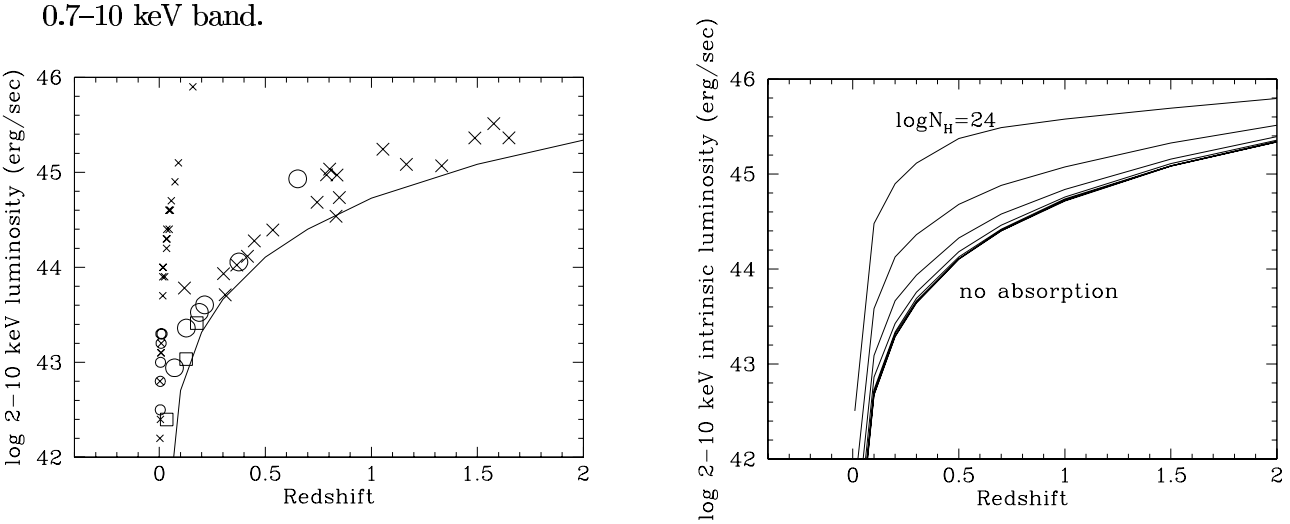

Fig. 2.— Left: 2–10 keV luminosity versus redshift. The HEAO-1 A2 AGN sample (Turner and Pounds 1989) is also shown with small marks. For the LSS sample, the luminosity is not corrected for intrinsic absorption. Marks are the same as in figure 1. Solid line is the detection limit for object without intrinsic absorption. Right: Detection limit to the intrinsic 2–10 keV luminosity as a function of redshift. From top to bottom, intrinsic column density of log N_H = 24.0, 23.5, 23.0, 22.5, 22.0, 21.5, 21.0, and no absorption with an intrinsic photon index of 1.7 were assumed. The survey limit of the SIS 3.5σ is 1.2 cts/ksec in the 2–7 keV band.

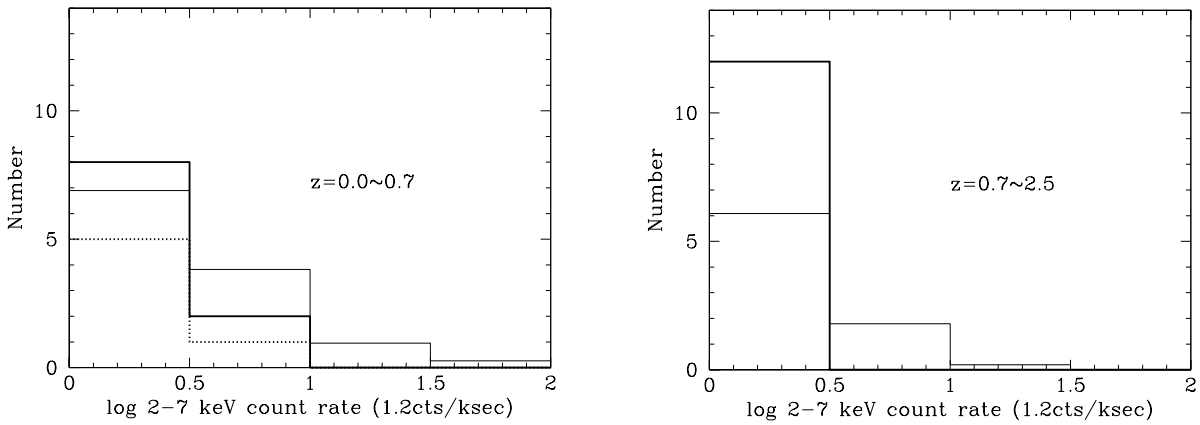

Fig. 3.— Detected number of AGN as a function of SIS count rate. The identified sample is divided at redshift of 0.7. Left: low redshift sample. Right: high redshift sample. Thick solid line represents type-1 plus type-1.5 AGNs and dotted line shows type-2 AGNs. Thin solid line shows expected number of type-1 AGNs derived from X-ray luminosity function of AGNs in the soft band (see section 4).

4. Deficiency of type-2 QSOs ?

X-ray luminosity vs. redshift of identified AGNs is shown in figure 2. (We also plotted AGNs in the HEAO-1 A2 sample (Turner and Pounds 1989) with small marks for comparison.) The number ratio between type-1 plus type-1.5 AGNs to type-2 AGNs is clearly changing with redshift, luminosity or both. In the next figure, detection limits to the intrinsic luminosity of objects with various absorption column density are shown as a function of redshift, for the SIS 3.5σ sample. We can unbiasly detect objects with intrinsic column density of up to $10^{22.5}/\mathrm{cm}^2$ in redshift smaller than 1.5 and up to $10^{23}/\mathrm{cm}^2$ in redshift larger than 1.5, thanks to the redshift effect. Thus, if the column density distribution of absorbing matter and the critical column density which divides type-1 and type-2 AGN changes with neither redshift nor luminosity, we expect the number ratio of type-2 to type-1 AGN does not change or become larger at higher redshift in our sample. The smaller number ratio at higher redshift supports the deficiency (e.g, Lawrence 1991) of so called "type-2 QSO", which is a narrow-line luminous AGN. It should be noted that there remains three sources which are unidentified in the SIS 3.5σ sample and these objects could be the missing high redshift type-2 AGNs.

To compare the redshift distribution of the identified AGNs with an AGN luminosity function and its evolution derived by ROSAT surveys, we divide the sample at redshift of 0.7. In figure 3, we show histograms of the detected number of type-1 plus type-1.5 and type-2 AGN as a function of SIS count rate. Expected numbers of AGNs using an AGN luminosity function derived from various ROSAT surveys (Hasinger 1998) is also shown. Since most of the ROSAT sample is type-1 AGN, we assumed the canonical photon index of 1.7 for type-1 AGNs to convert the 0.5–2 keV luminosity to SIS count rate. Detected number of type-1 plus type-1.5 AGN in the redshift range of 0.0–0.7 is consistent with the estimated number. While in redshift range of 0.7–2.5, the

detected number shows a small excess. This could be explained by an excess of QSOs at z=0.8 in our sample (see, figure 2). The number of type-2 AGNs in the low redshift sample is about half of the number of type-1 AGNs. On the other hand, there is no type-2 AGN in the high redshift sample as mentioned above.

Compilation of optical identifications of deep ASCA surveys will set more strict constraints on the change of the number ratio of type-2 to type-1 AGN with redshift and luminosity. However, XMM surveys, which cover flux limit range from comparable to to 100 times deeper than that of the LSS, are absolutely needed to qualitatively discuss cosmological evolutions of the luminosity functions of type-2 and type-1 AGN.

REFERENCES

Akiyama, M., et al. 1998, AN, 319, 63

Akiyama, M., et al. 1998, ApJ, 500, 173

Comastri, A., Setti, G., Zamorani, G., & Hasinger, G. 1995, A&A, 296, 1

Elvis, M., et al., 1994, ApJS, 95, 1

Gendreau, K.C., et al. 1995, PASJ, 47, L5

Gondek, D., et al. 1996, MNRAS, 282, 646

Hartwick, F.D.A., & Schade, D. 1990, ARA&A, 28, 437

Hasinger, G. 1998, AN, 319, 37

Lawrence, A. 1991, MNRAS, 252, 586

McMahon, R.G., Irwin, M.J., & Hazard, C. 1992, Gemini Issue, 36, 1

Schmidt, M., et al., 1998, A&A, 329, 495

Turner, T.J., Pounds, K.A. 1989, MNRAS, 240, 833

Ueda, Y., et al. 1998a, Nature, 391, 868

Ueda, Y., et al. 1998b, AN, 319, 47

Ueda, Y., et al. 1998c, ApJ, submitted

White, R.L., Becker, R.H., Helfand, D.J., & Gregg, M.D. 1997, ApJ, 475, 479

Voges, W., et al. 1998, in this proceeding